Universiteit
Leiden
The Netherlands

Enlightening the primordial dark ages

Iarygina, O.

Citation

Iarygina, O. (2021, November 3). *Enlightening the primordial dark ages*. *Casimir PhD Series*. Retrieved from https://hdl.handle.net/1887/3238935

Version:	Publisher's Version
License:	Licence agreement concerning inclusion of doctoral thesis in the Institutional Repository of the University of Leiden
Downloaded from:	https://hdl.handle.net/1887/3238935

Note: To cite this publication please use the final published version (if applicable).

3 Gravitational waves from spectator Gauge-flation

Abstract: We investigate the viability of inflation with a spectator sector comprised of non-Abelian gauge fields coupled through a higher order operator. We dub this model "spectator Gauge-flation". We study the predictions for the amplitude and tensor tilt of chiral gravitational waves and conclude that a slightly red-tilted tensor power spectrum is preferred with $n_T = -\mathcal{O}(0.01)$. As with related models, the enhancement of chiral gravitational waves with respect to the single-field vacuum gravitational wave background is controlled by the parameter $\gamma = g^2Q^2/H^2$, where g is the gauge coupling, H is the Hubble scale and Q is the VEV of the $SU(2)$ sector. The requirement that the $SU(2)$ is a spectator sector leads to a maximum allowed value for γ, thereby constraining the possible amplification. In order to provide concrete predictions, we use an α-attractor T-model potential for the inflaton sector. Potential observation of chiral gravitational waves with significantly tilted tensor spectra would then indicate the presence of additional couplings of the gauge fields to axions, like in the spectator axion-SU(2) model, or additional gauge field operators.

Keywords: physics of the early universe, inflation, primordial gravitational waves, gravitational waves and CMBR polarization.

Based on:

O. Iarygina and E. I. Sfakianakis
Gravitational waves from spectator Gauge-flation
arXiv:2105.06972.

3.1 Introduction

Inflation provides an elegant solution for the horizon and flatness problems, as well as a mechanism for producing density fluctuations in very good agreement with the latest observational tests. Typically, scalar fields play a major role in inflationary model-building since they do not spoil the homogeneity and isotropy of the background cosmology. However, models of particle physics generically include also gauge fields and their presence in the inflationary epoch may significantly influence cosmological predictions. Scalar perturbations that are produced during inflation are tightly constrained by observations [220], while the primordial tensor modes (generated as primordial gravitational waves) are still not detected. The primordial Stochastic Gravitational Wave Background (SGWB) is a unique test of the physics of the very early Universe, that could provide signatures of the particle content and the energy scale of inflation. Nowadays, the search for primordial gravitational waves (GWs) is mainly focused [221, 222] on the parity-odd polarization pattern in the CMB the B-modes. A correct interpretation of B-mode measurements strongly relies on understanding their production mechanism.

One intriguing scenario is GW generation by gauge fields. Gauge field tensor modes can experience a tachyonic growth in one of their polarizations, leading to production of chiral GWs. In addition to chirality, produced GWs may be significantly red or blue tilted and non-Gaussian. One of the very-well known models of inflation, where non-Abelian gauge fields generate accelerated expansion, is the Gauge-flation model that was originally proposed in Refs. [74, 75]. Gauge-flation is related to Chromo-Natural inflation [223] that contains an axion coupled to $SU(2)$ gauge fields. Gauge-flation can be formally obtained from chromo-natural inflation after integrating out an axion field near the minimum of the axion potential [76, 224–226]. The original formulation of both models is ruled out by *Planck* observations [227–230]. However, both models can be made consistent with current CMB bounds if the gauge symmetry is spontaneously broken by a Higgs sector [231, 232]. Interestingly Higgsed gauge-flation and Higgsed Chromo-natural inflation give somewhat different predictions for the shape of the produced GW spectrum.

Recent interest in potentially distinguishable signatures from the standard vacuum fluctuations by future B-mode experiments, like LiteBIRD, has led to a number of generalizations of gauge-field-driven GW models. In particular considering a spectator axion sector coupled to non-abelian

gauge fields has significantly opened up the parameter space [233–237]. It was recently demonstrated [238] that Chromo-Natural inflation as a spectator sector for the scalar single-field inflation can be in agreement with the current data, while at the same time generating potentially distinguishable observable signatures for the tensor modes. In Ref. [239] it was shown that in spectator Chromo-Natural inflation, depending on the choice of the axion potential, all three possible tensor tilts may be generated: flat, red and blue. In addition to that, peaked or oscillating GW spectra are also possible for well-motivated axion potentials. Since in Gauge-flation there is much less freedom due to the absence of the axion field, a question arises: what are the possible GW spectra arising from a spectator Gauge-flation sector?

In this work we demonstrate the viability of the spectator Gauge-flation scenario, study its predictions and limitations and also provide a comparison with predictions of related models. The paper is organised as follows: In Section 3.2 we introduce the framework for non-Abelian gauge field inflation and then embed it as a spectator sector for scalar single-field inflation. In Section 3.3 we discuss the necessary conditions for the $SU(2)$ sector to be subdominant, as compared to the inflaton sector. This ensures that the scalar fluctuations will be dominated by the inflaton sector and can be made to agree with the observational constraints, for example by considering an α-attractor inflationary potential. Keeping the non-Abelian sector subdominant leads to an upper bound for the amplitude enhancement of the tensor power spectra. In Section 3.4 we discuss predictions for the primordial tensor tilt and it's dependence on the parameters of the theory. We use a well-known α-attractor model as the inflaton sector, since it can provide an arbitrarily low amount of vacuum-generated GWs (at least in principle), while at the same time obeying the constraints for the scalar fluctuations. We conclude in Section 3.5.

3.2 Framework

3.2.1 The model

In this section we describe the theory of Gauge-flation and its embedding as a spectator sector for inflation. The Gauge-flation action is given by [74, 75]

$$S = \int d^4x \sqrt{-\det(g_{\mu\nu})} \left[\frac{M_{\rm Pl}^2}{2} R - \frac{1}{4} F^a_{\mu\nu} F^{a\,\mu\nu} + \frac{\kappa}{96} \left(F^a_{\mu\nu} \tilde{F}^{a\,\mu\nu} \right)^2 \right], \quad (3.1)$$

where R is the space-time Ricci scalar, $F^a_{\mu\nu} = \partial_\mu A^a_\nu - \partial_\nu A^a_\mu - g\epsilon^{abc}A^b_\mu A^c_\nu$ is the field strength of an $SU(2)$ gauge field A^a_μ, $\tilde{F}^{a\,\mu\nu} = \epsilon^{\mu\nu\rho\sigma}F^a_{\rho\sigma}/\left(2\sqrt{-\det(g_{\mu\nu})}\right)$ its dual (where $\epsilon^{\mu\nu\alpha\beta}$ is the antisymmetric tensor and $\epsilon^{0123} = 1$), $\kappa > 0$ is a parameter with dimension $M_{\rm pl}^{-4}$ and g is the gauge field coupling.

We will work with the FLRW metric

$$ds^2 = -dt^2 + a(t)^2\delta_{ij}dx^i dx^j, \tag{3.2}$$

where i, j indicate the spatial directions. An isotropic solution for the background is given by the following configuration of the gauge field

$$A^a_0 = 0, \tag{3.3}$$
$$A^a_i = \delta^a_i a(t)Q(t) \tag{3.4}$$

and it has been shown to be an attractor solution [75]. For this ansatz the closed system of equations for the vacuum expectation value (VEV) of the gauge field $Q(t)$ and the Hubble parameter $H(t)$ is given by

$$M^2_{\rm Pl}\dot{H} = -\left((\dot{Q} + HQ)^2 + g^2Q^4\right) \tag{3.5}$$
$$M^2_{\rm Pl}H^2 = \frac{1}{2}\left((\dot{Q} + HQ)^2 + g^2Q^4 + \kappa g^2Q^4(\dot{Q} + HQ)^2\right), \tag{3.6}$$
$$\left(1 + \kappa g^2Q^4\right)\left(\ddot{Q} + 3H\dot{Q} + \dot{H}Q\right) + 2g^2Q^3\left(1 + \kappa\dot{Q}^2\right) + 2H^2Q = 0, \tag{3.7}$$

where an overdot denotes a derivative with respect to cosmic time t.

We now introduce a scalar field $\varphi(t)$ with a potential $V(\varphi)$ that is responsible for driving inflation and consider the Gauge-flation terms as a spectator sector, i.e.

$$S = \int d^4x\sqrt{-\det(g_{\mu\nu})}\left[\frac{M^2_{\rm Pl}}{2}R - \frac{1}{2}(\partial\varphi)^2 - V(\varphi) - \frac{1}{4}F^a_{\mu\nu}F^{a\,\mu\nu} + \frac{\kappa}{96}\left(F^a_{\mu\nu}\tilde{F}^{a\,\mu\nu}\right)^2\right]. \tag{3.8}$$

Up to gravitational interactions the dynamics of the inflaton sector is completely decoupled from the dynamics of the gauge field. This allows the inflaton field $\varphi(t)$ to be responsible for the predictions for scalar fluctuations. At the same time the gravitational waves generated by the gauge field sector can lead to observable signatures in the tensor power spectra. In this paper we will not consider scalar fluctuations and refer to Ref. [233] where scalar fluctuations were studied for a related model, where the spectator sector involved an axion coupled to an $SU(2)$ field through a Chern-Simons term (which we call spectator Chromo-natural inflation). A recent

analysis of scalar fluctuations, including non-linear effects, can be found in Refs. [240, 241]. We expect that the bounds on tensor modes arising from the spectator nature of the Gauge-flation sector will result in subdominant density fluctuations from it. We will thus focus our attention solely on the tensor sector, leading to the production of GW's.

Using the ansatz of Eq. (3.4) the background system of equations in the presence of the inflaton field changes to

$$M_{\rm Pl}^2\dot{H} = -\left((\dot{Q}+HQ)^2+g^2Q^4\right)-\frac{1}{2}\dot{\varphi}^2, \tag{3.9}$$

$$M_{\rm Pl}^2H^2 = \frac{1}{3}\left(\frac{1}{2}\dot{\varphi}^2+V(\varphi)\right)+\frac{1}{2}\left((\dot{Q}+HQ)^2+g^2Q^4+\kappa g^2Q^4(\dot{Q}+HQ)^2\right), \tag{3.10}$$

$$\left(1+\kappa g^2Q^4\right)\left(\ddot{Q}+3H\dot{Q}+\dot{H}Q\right)+2g^2Q^3\left(1+\kappa\dot{Q}^2\right)+2H^2Q=0, \tag{3.11}$$

$$\ddot{\varphi}+3H\dot{\varphi}+V_\varphi(\varphi)=0, \tag{3.12}$$

where $V_\varphi(\varphi)=\partial V(\varphi)/\partial\varphi$. The standard Hubble slow roll parameters are defined as

$$\epsilon=-\frac{\dot{H}}{H^2},\quad \eta=-\frac{\ddot{H}}{2H\dot{H}}=\epsilon-\frac{\dot{\epsilon}}{2\epsilon H}. \tag{3.13}$$

The slow-roll parameter ϵ contains contributions from the scalar (inflaton) and the gauge field (spectator) sectors. The various contributions can be written as

$$\epsilon=\epsilon_\varphi+\epsilon_{Q_E}+\epsilon_{Q_B}, \tag{3.14}$$

where

$$\epsilon_\varphi=\frac{\dot{\varphi}^2}{2M_{\rm Pl}^2H^2},\quad \epsilon_{Q_E}=\frac{(\dot{Q}+HQ)^2}{M_{\rm Pl}^2H^2},\quad \epsilon_{Q_B}=\frac{g^2Q^4}{M_{\rm Pl}^2H^2}. \tag{3.15}$$

Throughout this work we assume – and check – that the inflaton field $\varphi(t)$ dominates the energy budget of the theory. This translates into the conditions $\epsilon_\varphi \gg \epsilon_Q$, where $\epsilon_Q=\epsilon_{Q_E}+\epsilon_{Q_B}$, and hence $\epsilon\simeq\epsilon_\varphi$. Despite this regime of interest, we keep the analytic part of our analysis as general as possible and clearly state the approximations wherever they are necessary for making analytical progress.

Although the inflationary era is dominated by $\varphi(t)$, in the same way as in the original Gauge-flation approach we will assume that the gauge field

also slow-rolls together with the inflaton field[1]. Hence for the later analysis we define

$$\delta = -\frac{\dot{Q}}{HQ}, \quad \gamma = \frac{g^2 Q^2}{H^2}. \tag{3.16}$$

We will require $\delta \ll 1$ to ensure that the gauge field slow-rolls long enough, to secure the needed amount of e-folds for inflation. The parameter γ is a characteristic quantity of the model. It was shown in Ref. [227] that for $\gamma < 2$ the scalar perturbations are tachyonically unstable. We thus restrict our analysis to the stable region with $\gamma > 2$. For the tensor sector this parameter characterises the enhancement of one of the polarizations for the tensor perturbation with respect to the gravitational wave background coming from the inflaton sector. So far there were no theoretical upper bounds on this parameter, only the observational constraints coming from the tensor-to-scalar ratio r. As we will see in the next subsection, for spectator Gauge-flation there exists an upper bound $\gamma_{\rm max}$ which is determined solely from the self-consistency of the theory and the slow-roll conidtions. For a given set of parameters g, ϵ and H, the upper bound on γ allows for an estimation of the maximal enhancement for the tensor power spectra and thus a theoretical upper bound on r.

3.2.2 Background parameters

In this subsection we will collect all the expressions for the background parameters that will be relevant for the tensor power spectra computation. To start with, there are two equivalent ways to write down the first slow-roll parameter in terms of background quantities. The first one follows directly from Eqs. (3.9) and (3.13), i.e.

$$\epsilon = \frac{1}{M_{\rm Pl}^2} Q^2 \left((1-\delta)^2 + \gamma \right) + \epsilon_\varphi. \tag{3.17}$$

Another way is to use the combination $\dot{H} + 2H^2$, which through Eqs. (3.9), (3.10) leads to

$$\epsilon = 2 - \frac{\kappa g^2 Q^6}{M_{\rm Pl}^2} (1-\delta)^2 + \frac{1}{3}\epsilon_\varphi - \Upsilon \,. \tag{3.18}$$

[1] A fast-rolling spectator gauge-flation sector can also lead to GW production. However, some fine-tuning is required to bring it in the observable window. We thus do not pursue this regime further.

We have defined

$$\Upsilon = \frac{2V}{3M_{\rm Pl}^2 H^2}\,, \tag{3.19}$$

which is determined by the scalar field inflation potential and can be taken to be approximately constant for slow-roll models of inflation. From Eqs. (3.13) and (3.17) we derive the second slow-roll parameter

$$\eta = \frac{Q^2}{M_{\rm Pl}^2}\left((1-\delta)^2 + (1-\delta)\frac{\dot\delta}{\epsilon H} + \gamma\frac{\delta}{\epsilon}\right) + \delta - \frac{\epsilon_\varphi}{\epsilon}\left(\delta - \eta_\varphi\right), \tag{3.20}$$

with $\eta_\varphi = -\frac{\ddot\varphi}{H\dot\varphi}$. An alternative derivation follows from Eqs. (3.13) and (3.18)

$$\begin{aligned}\eta = \epsilon - (2 - \Upsilon - (\epsilon - \frac{1}{3}\epsilon_\varphi))\left(\frac{\dot\delta}{H\epsilon(1-\delta)} + \frac{3\delta}{\epsilon}\right) - \frac{\epsilon_\varphi}{3}\left(1 - \frac{\eta_\varphi}{\epsilon}\right) + \\ + \frac{2}{3}\left(\frac{\epsilon_\varphi V_\varphi}{\dot\varphi H\epsilon} + \frac{V}{H^2 M_{\rm Pl}^2}\right).\end{aligned} \tag{3.21}$$

Up to now the above equations are exact. If the inflaton is assumed to dominate the total energy budget, Eq. (3.20) leads to $\eta \simeq \frac{\epsilon_\varphi}{\epsilon}\eta_\varphi$. Substituting that into Eq. (3.21) and neglecting[2] $\frac{\dot\delta}{H(1-\delta)}$, we find

$$\delta \simeq \frac{\epsilon}{3(2 - \Upsilon - (\epsilon - \frac{1}{3}\epsilon_\varphi))}\left(\epsilon - \frac{2}{3}\frac{\epsilon_\varphi}{\epsilon}\eta_\varphi - \frac{\epsilon_\varphi}{3} + \Upsilon\left(1 - \frac{\epsilon_\varphi}{\epsilon}\right)\right), \tag{3.22}$$

where we have used $\epsilon_V = \frac{M_{\rm Pl}^2}{2}\left(\frac{V_\varphi}{V}\right)^2 \simeq \epsilon_\varphi$ and $\dot\varphi = -HM_{\rm Pl}\sqrt{2\epsilon_\varphi}$ is chosen to be negative without loss of generality.

In addition to that, Eqs. (3.16) and (3.18) we find

$$\kappa = \frac{1}{H^2\gamma Q^2}\frac{(1-\delta)^2 + \gamma}{(1-\delta)^2}\frac{2 - \left(\epsilon_Q + \frac{2}{3}\epsilon_\varphi + \Upsilon\right)}{\epsilon_Q}. \tag{3.23}$$

Moreover, from Eq. (3.17) one may derive the relation that will help to eliminate $M_{\rm Pl}$ from the equations

$$M_{\rm Pl} = Q\sqrt{\frac{(1-\delta)^2 + \gamma}{\epsilon_Q}}, \tag{3.24}$$

[2]The arguments for neglecting this term are discussed in Ref. [75]. We numerically checked the validity of this approximation

where ϵ_Q is the first slow-roll parameter for the gauge field sector, i.e. $\epsilon_Q = \epsilon_{Q_E} + \epsilon_{Q_B}$. The relations above with the inflaton sector set to zero coincide with relations obtained in Ref. [227], which provides a consistency check for our analysis. Eq. (3.22) was derived strictly under the assumption of a dominant inflaton sector and thus does not reduce to the gauge-flation result for $\epsilon_\phi \to 0$, which is not true for all equations before it, which are exact and hence applicable to any gauge-flation scenario, with or without a separate inflaton sector.

Finally, from Eqs. (3.16) and (3.17) we find that for $\delta \ll 1$

$$1 - \frac{\epsilon_\varphi}{\epsilon} \simeq \frac{H^2}{M_{\rm Pl}^2 g^2 \epsilon}\gamma(\gamma+1). \tag{3.25}$$

From Eq. (3.25) we obtain γ as a function of ϵ and ϵ_φ

$$\gamma \simeq -\frac{1}{2} + \frac{1}{2}\sqrt{1 + 4M_{\rm Pl}^2 \frac{g^2\epsilon}{H^2}\left(1 - \frac{\epsilon_\varphi}{\epsilon}\right)}. \tag{3.26}$$

The dependence of γ on $\epsilon_\varphi/\epsilon$ is shown in Fig. (3.1). Since $0 < \epsilon_\varphi < \epsilon$, the right hand side of Eq. (3.25) is in the range $0 < \frac{H^2}{M_{\rm Pl}^2 g^2 \epsilon}\gamma(\gamma+1) < 1$. Hence, the maximum value of the parameter γ is

$$\gamma_{\rm max} = -\frac{1}{2} + \frac{1}{2}\sqrt{1 + 4M_{\rm Pl}^2 \frac{g^2\epsilon}{H^2}}\,. \tag{3.27}$$

The result of Eq. (3.27) is obtained without the requirement $\epsilon \simeq \epsilon_\varphi$ and is rather generic. One can see that the parameter γ cannot be chosen arbitrarily high any more, but reaches its maximal value given by Eq. (3.27) due to the restrictions of the theory. The maximum value of γ is achieved when the energy budget is completely controlled by the gauge sector, i.e. when $\frac{\epsilon_\varphi}{\epsilon} \ll 1$, meaning that ϵ is dominated by ϵ_Q. In the spectator case $\epsilon \simeq \epsilon_\varphi$, and γ is limited to a smaller range of values, with a magnitude that depends only on g (with fixed H and ϵ). Interestingly enough, this allows us to find the minimum allowed value of the gauge coupling $g_{\rm min}$ for spectator Gauge-flation. Simply from the stability condition of scalar perturbations[3] $\gamma_{\rm max} > 2$ we obtain

$$g_{\rm min} > \sqrt{\frac{6}{M_{\rm Pl}\,\epsilon}}H. \tag{3.28}$$

[3]For $\gamma_{\rm max} < 2$ scalar perturbations experience a tachyonic instability, see [227] for a detailed discussion.

We can estimate the value of $g_{\rm min}$ by relating H and ϵ to the amplitude of the scalar power spectrum $P_\zeta = \frac{H^2}{8\pi^2 M_{\rm Pl}^2 \epsilon} \simeq 2.2 \times 10^{-9}$, since we assume that the scalar power spectrum is dominated by the fluctuations in the inflaton sector. This results in $g_{\rm min} \simeq 4\pi\sqrt{3P_\zeta} \simeq 0.001$. Then $\gamma_{\rm max}$ may be estimated as $\gamma_{\rm max} \simeq -\frac{1}{2} + \frac{1}{2}\sqrt{1 + \frac{g^2}{2\pi^2 P_\zeta}} \simeq 15$ for $g = 6.5 \times 10^{-3}$. The dependence of $\gamma_{\rm max}$ on the value of g is shown in Fig. (3.1). A complementary method for computing the maximum allowed tensor amplification based on the back-reaction of the produced spin-2 particles was presented in Ref. [242].

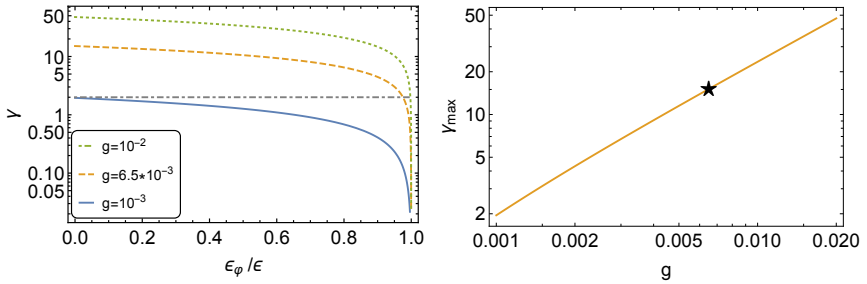

Figure 3.1: *Left:* The dependence of γ on $\epsilon_\varphi/\epsilon$ for $g = 10^{-3}, 6.5 \times 10^{-3}, 10^{-2}$ (blue-solid, orange-dashed and green-dotted lines respectively) and $H = 1.9 \times 10^{-6} M_{\rm pl}, \epsilon = 2 \times 10^{-5}$. The dot-dashed grey line shows the lower bound for the parameter, $\gamma = 2$. *Right:* The dependence of $\gamma_{\rm max}$ on the gauge coupling g for the same values of H and ϵ as on the left plot. The star represents the value of $g = 6.5 \times 10^{-3}$ that we use in our numerical simulations in the subsequent sections, unless stated otherwise.

3.3 Viability of spectator Gauge-flation

In this section we will show the viability of the spectator Gauge-flation. We will consider and discuss the most important dynamics on the example of an α-attractor potential for the inflaton field. To ensure that the gauge sector of Eq. (3.8) is a spectator sector, the energy density of the gauge fields must be subdominant to that of the inflaton

$$\rho_\varphi \gg \rho_{Q_E},\ \rho_{Q_B},\ \rho_{Q_\kappa}, \tag{3.29}$$

where the definitions for the energy densities are given as [74]

$$\rho_\varphi = \frac{1}{2}\dot{\varphi}^2 + V(\varphi), \tag{3.30}$$

$$\rho_{Q_E} = \frac{3}{2}(\dot{Q} + HQ)^2, \tag{3.31}$$

$$\rho_{Q_B} = \frac{3}{2}g^2Q^4, \tag{3.32}$$

$$\rho_{Q_\kappa} = \frac{3}{2}\kappa g^2Q^4(\dot{Q} + HQ)^2. \tag{3.33}$$

A similar condition must hold for the first slow-roll quantity ϵ

$$\epsilon_\varphi \gg \epsilon_{Q_E}, \epsilon_{Q_B}, \tag{3.34}$$

meaning that the Hubble evolution is dominated by the rolling of the inflaton field (see eq. (3.15)). The above inequalities can be re-cast as relations between the VEVs of the inflaton and gauge fields

$$\frac{1}{2}\dot{\varphi}^2 \gg (\dot{Q} + HQ)^2, \tag{3.35}$$

$$\frac{1}{2}\dot{\varphi}^2 \gg g^2Q^4, \tag{3.36}$$

$$\frac{1}{2}\dot{\varphi}^2 + V(\varphi) \gg \frac{3}{2}(\dot{Q} + HQ)^2 \tag{3.37}$$

$$\frac{1}{2}\dot{\varphi}^2 + V(\varphi) \gg \frac{3}{2}g^2Q^4, \tag{3.38}$$

$$\frac{1}{2}\dot{\varphi}^2 + V(\varphi) \gg \frac{3}{2}\kappa g^2Q^4(\dot{Q} + HQ)^2. \tag{3.39}$$

Let us note that for spectator Chromo-natural inflation precisely the same inequalities of Eq. (3.37) and (3.38) should hold, in addition to an inequality for the axion field $\chi(t)$, i.e. $\frac{1}{2}\dot{\varphi}^2 + V(\varphi) \gg \frac{1}{2}\dot{\chi}^2 + U(\chi)$ that replaces Eq. (3.39) since the κ-term can be thought as the analogue of the axion potential in Chromo-natural inflation.

From Eqs. (3.35) – (3.39) one may see that $\epsilon_\varphi \gg \epsilon_{Q_E}, \epsilon_{Q_B}$ implies $\rho_\varphi \gg \rho_{Q_E}$, ρ_{Q_B}, as well as $\rho_\varphi \gg \rho_{Q_\kappa}$, if κ is not too large. Hence, Eqs. (3.37) and (3.38) as well as Eq. (3.39) hold automatically when Eqs. (3.35) and (3.36) are satisfied. Therefore we will focus on showing the allowed parameter ranges to satisfy $\epsilon_\varphi \gg \epsilon_{Q_E}, \epsilon_{Q_B}$, i.e. Eqs. (3.35) and (3.36), and confirm our findings with numerical simulations.

For illustrative purposes we will consider an α-attractor model for the inflaton sector [50, 243–245]. It is known that the universal predictions for

the spectral index n_s and tensor-to-scalar ratio r are in agreement with the latest *Planck* data [220]. They are parametrised solely by the dimensionless coupling $\tilde{\alpha}$ and the number of e-folds N_* before the end of inflation when the CMB modes exit the horizon during inflation, i.e.

$$n_s = 1 - \frac{2}{N_*}, \quad r = \frac{12\tilde{\alpha}}{N_*^2}. \tag{3.40}$$

The α-attractor T-model potential is given by

$$V(\phi) = \tilde{\alpha}\tilde{\mu}^2 M_{\rm Pl}^2 \left((\tanh(\tilde{\beta}\phi/2))^2\right)^n, \tag{3.41}$$

where the parameters of the potential are chosen to be

$$\tilde{\beta} = \sqrt{2/3\tilde{\alpha}}, \quad n = 3/2, \quad \tilde{\alpha} = 0.1, \quad \tilde{\mu}^2 = 1.08 \times 10^{-10} M_{\rm Pl}^2, \tag{3.42}$$

and are used for numerical simulations in this section. For the gauge sector we use[4]

$$\begin{gathered} g = 6.5 \times 10^{-3}, \quad \kappa = 1.733 \times 10^{20} M_{\rm Pl}^{-4}, \\ \dot{Q}_0/M_{\rm pl}^2 = -10^{-10}, \quad Q_0/M_{\rm pl} = 7 \times 10^{-4}, 10^{-3}, 1.5 \times 10^{-3}, \end{gathered} \tag{3.43}$$

where $Q_0, \dot{Q}_0$ are initial value and initial velocity respectively for the gauge field VEV.

For given parameters one may numerically evolve the system of Eqs. (3.9) – (3.12) and find that, indeed, it is possible to satisfy the conditions of Eqs. (3.29) and (3.34). Fig. (3.2) shows the evolution of the inflaton field $\varphi(N)$ and VEV of the gauge field $Q(N)$ as a function of the number of e-folds N. Notice that $Q(N)$ evolves mildly with N and stays almost constant. The shape of the parameter $\gamma(N)$ which is defined in Eq. (3.16) mimics the behaviour of $Q(N)$ which is shown on Fig. (3.4). As we will see in Section 3.4.2, the shape of γ determines the tilt of the tensor power spectrum. Since we require that $Q(N)$ also slow-rolls during the slow-roll of $\varphi(N)$, we expect $\gamma(N)$ to be a decreasing function of time[5]. The evolution of the components of ϵ and ρ is shown on Fig. (3.3). As we have seen in our numerical simulations, for α-attractors the most restrictive condition

[4]The naturalness of the κ-term and its domination over all the other dimension eight or higher contributions coming from gauge field or fermionic loops is discussed in Ref. [76]. Also note that $\kappa^{-1/4} > H_{\rm infl.}$.

[5]The post-inflationary dynamics and the effect of parametric resonance [158–160] is left for future work.

to host a Gauge-flation sector as a spectator for inflation appears to be the condition $\epsilon_\varphi \gg \epsilon_{Q_B}$. It is known (see e.g. Refs. [50, 158]), that for α-attractors $\epsilon_\varphi \simeq \frac{3\tilde{\alpha}}{4N^2}$. Hence, with the definitions of Eqs. (3.15) and (3.16), $\epsilon_\varphi \gg \epsilon_{Q_B}$ is satisfied for

$$\frac{3\tilde{\alpha}}{4N^2} \gg \frac{\gamma Q^2}{M_{\rm Pl}^2}. \tag{3.44}$$

By fixing the parameter $\tilde{\alpha}$, the number of e-folds N and the value of $\gamma > 2$, it is easy to find the range of allowed initial values for the gauge field Q_0, in order for the non-Abelian sector to stay subdominant. One may rewrite the condition of Eq. (3.44) using Eq. (3.16) and $H^2 \simeq H_\varphi^2 \simeq \frac{\tilde{\alpha}\tilde{\mu}^2}{3}$ in the following form

$$\frac{3M_{\rm Pl}}{2\tilde{\mu}N} \gg \frac{\gamma}{g}. \tag{3.45}$$

Similarly, the condition $\epsilon_\varphi \gg \epsilon_{Q_E}$ may be written for $\delta \ll 1$ using Eqs. (3.15), (3.16) as

$$\frac{3M_{\rm Pl}}{2\tilde{\mu}N} \gg \frac{\sqrt{\gamma}}{g}. \tag{3.46}$$

Indeed, we see that the condition $\epsilon_\varphi \gg \epsilon_{Q_B}$ is more restrictive, which agrees with our numerical simulations. The left-hand side of Eqs. (3.45), (3.46) is a fixed number that is set by the number of e-folds of inflation N and the scale $\tilde{\mu}$, that does not depend on the parameters of the potential $\tilde{\alpha}$ and n, and is uniquely fixed from the amplitude of the power spectrum of the scalar density perturbations. The range for allowed values for γ and g that satisfy Eq. (3.45) is shown in Fig. 3.5.

3.4 Tensor sector

In this Section we will analyze the tensor perturbations generated by the gauge fields. We will explicitly identify restrictions in the parameter space coming from the inflaton sector on the gravitational wave production by the gauge sector.

3.4.1 Tensor perturbations

In this subsection we adopt the notation of Ref. [233] for tensor perturbations in the gauge field and the metric. The tensor sector consists of four independent perturbations that are given by

$$\begin{aligned} \delta A_\mu^1 = &\quad a(0, t_+, t_\times, 0), \quad \delta A_\mu^2 = a(0, t_\times, -t_+, 0), \\ \delta g_{11} = &\quad -\delta g_{22} = a^2 h_+, \quad \delta g_{12} = a^2 h_\times. \end{aligned} \tag{3.47}$$

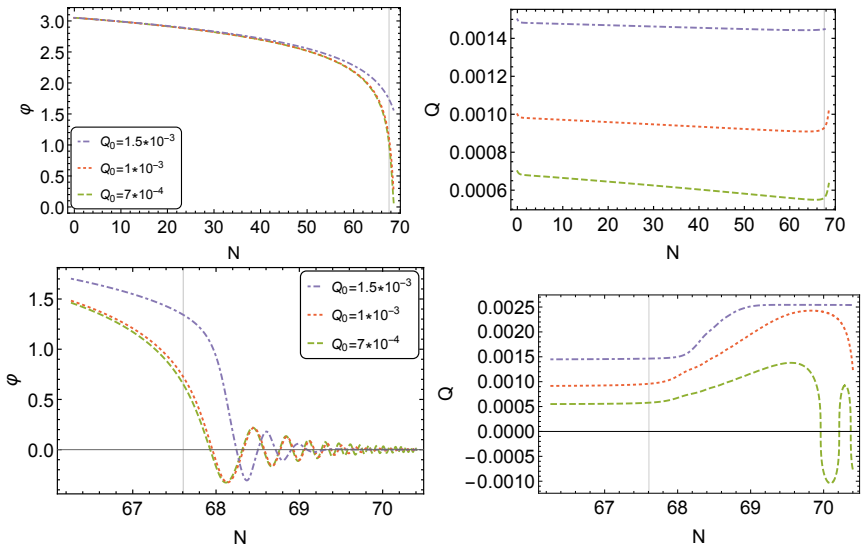

Figure 3.2: *Upper left:* The dependence of the inflaton field φ on the e-folding number N for the α-attractor T-model potential of Eq. (3.41) for $Q_0/M_{\rm pl} = 7\times10^{-4}, 1\times10^{-3}, 1.5\times10^{-3}$ (green-dashed, red-dotted and purple-dot-dashed lines respectively). The vertical grey grid line shows the end of inflation. *Upper right:* The dependence of the gauge field VEV Q on the e-folding number N for the same potential and color coding. The solid grey grid line shows the end of inflation. *Lower Left:* The evolution of the inflaton field φ after the end of inflation for the same parameters and color-coding. Lower right: The post-inflationary evolution of the gauge field VEV Q for the same parameters and color-coding.

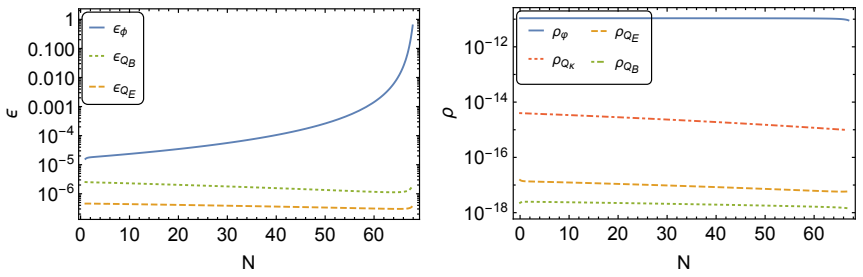

Figure 3.3: *Left:* The evolution of components of the first slow-roll parameter ϵ with the number of e-folds N for $Q_0/M_{\rm pl} = 7\times10^{-4}$. *Right:* The evolution of components of the energy-density ρ with the number of e-folds N for the same parameters.

The plus and cross polarizations are related to the left-handed and right-handed polarizations as

$$\begin{aligned} h_+ &= \frac{h_L + h_R}{\sqrt{2}}, \quad h_\times = \frac{h_L - h_R}{i\sqrt{2}}, \\ t_+ &= \frac{t_L + t_R}{\sqrt{2}}, \quad t_\times = \frac{t_L - t_R}{i\sqrt{2}}. \end{aligned} \tag{3.48}$$

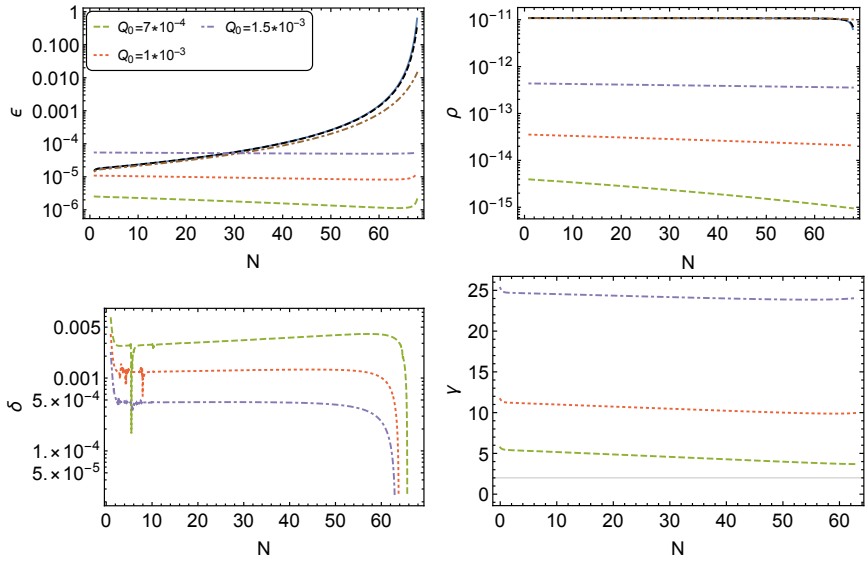

Figure 3.4: *Top left:* Components ϵ_{Q_B} as a function of the e-folding number N for $Q_0/M_{\rm pl} = 7\times10^{-4}, 1\times10^{-3}, 1.5\times10^{-3}$ (green-dashed, red-dotted and purple-dot-dashed lines respectively). The blue-solid, black-dashed and brown-dot-dashed and curved correspond to ϵ_φ for $Q_0/M_{\rm pl} = 7\times10^{-4}, 1\times10^{-3}, 1.5\times10^{-3}$ respectively. One can see that indeed $\gamma_{\rm max} \simeq 15$ is the maximally possible value for Gauge-flation to stay in the spectator sector for the given set of parameters. *Top right:* Components ρ_κ and their dependence on N for Q_0 and color-coding. The very top curves correspond to ρ_φ and are practically indistinguishable. *Bottom row:* The evolution of the parameter δ (left) and γ (right) for the same parameters and color-coding. The solid grey grid line on the right panel shows the bound $\gamma = 2$, below which scalar fluctuations in the theory are unstable.

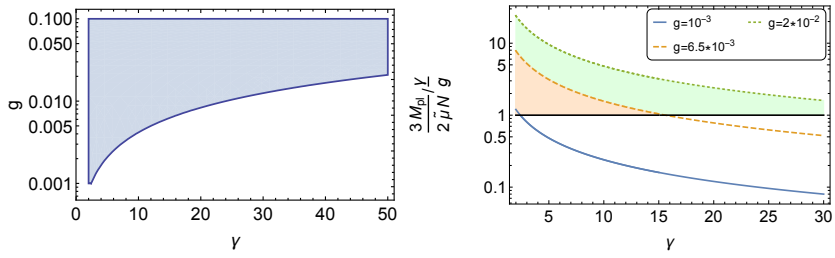

Figure 3.5: *Left:* The region plot for γ and g that satisfies Eq. (3.45) for $N = 60$. *Right:* The ratio $\frac{3M_{\rm Pl}}{2\tilde{\mu}N}/\frac{\gamma}{g}$ as a function of γ for $N = 60$ and $g = 10^{-3}, 6.5\times10^{-3}, 2\times10^{-2}$ (blue-solid, orange-dashed and green-dotted lines respectively). The black grid line shows when the ratio equals to 1.

We canonically normalise them by introducing

$$h_{L,R} = \frac{\sqrt{2}}{M_p a} H_{L,R}, \quad t_{L,R} = \frac{1}{\sqrt{2}a} T_{L,R}, \tag{3.49}$$

The action for canonically normalised perturbations reads

$$S_L = \frac{1}{2}\int d\tau d^3k \left[\Delta_L'^{\dagger}\Delta_L' + \Delta_L'^{\dagger} K_L \Delta_L - \Delta_L^{\dagger} K_L \Delta_L' - \Delta_L^{\dagger}\Omega_L^2 \Delta_L\right], \; \Delta_L = \begin{pmatrix} H_L \\ T_L \end{pmatrix}. \tag{3.50}$$

where the expression for the right-handed sector is identical. Prime $()'$ here denotes a derivative with respect to conformal time τ. The anti-symmetric matrix $K_{L/R}$ is defined through

$$K_{L/R,12} = \frac{1}{M_p}\left(Q' + \frac{a'}{a}Q\right), \tag{3.51}$$

and $\Omega^2_{L/R}$ is symmetric, with components

$$\Omega^2_{L/R,11} = k^2 - 2\frac{a'^2}{a^2} + \frac{3g^2a^2Q^4}{M_p^2} - \frac{(aQ)'^2}{M_p^2 a^2}, \tag{3.52}$$

$$\Omega^2_{L/R,12} = \pm k\frac{2gaQ^2}{M_p} + \frac{(aQ)'}{aM_p}\frac{a'}{a} - \frac{2\kappa g^2 Q^3}{M_p a^2}\frac{g^2a^4Q^4 + a'^2Q^2 - a^2Q'^2}{1+\kappa g^2 Q^4}, \tag{3.53}$$

$$\Omega^2_{L/R,22} = k^2 \mp 2kgaQ\left[1 + \kappa\frac{g^2a^4Q^4 + a'^2Q^2 - a^2Q'^2}{a^4(1+\kappa g^2Q^4)}\right] + \\ + \frac{2\kappa g^2Q^2}{a^2}\frac{g^2a^4Q^4 + a'^2Q^2 - a^2Q'^2}{1+\kappa g^2Q^4}, \tag{3.54}$$

where signs refer to the left-handed or the right-handed polarization respectively, which we denote by "L/R". Now, we are going to use the background relations obtained in Section 3.2.2 to simplify the above matrix elements and expand them in slow-roll in order to identify limitations on the chiral gravitational wave production, coming from the presence of the inflaton field. It is convenient to rewrite the matrices in terms of ϵ, γ and δ. With substitutions coming from Eqs. (3.16), (3.23) and (3.24)

$$Q' \to -aQH\delta \quad , \quad a' \to a^2H \quad , \quad \kappa \to \frac{1}{H^2\gamma Q^2}\frac{(1-\delta)^2+\gamma}{(1-\delta)^2}\frac{2-\left(\epsilon_Q + \frac{2}{3}\epsilon_\varphi + \Upsilon\right)}{\epsilon_Q}, \tag{3.55}$$

$$M_p \to Q\sqrt{\frac{(1-\delta)^2+\gamma}{\epsilon_Q}} \quad , \quad g \to \sqrt{\gamma}\frac{H}{Q}, \tag{3.56}$$

we find exact expressions for the matrices given by

$$K_{L/R,12} = \frac{aH\sqrt{\epsilon_Q}}{\sqrt{(1-\delta)^2+\gamma}}(1-\delta), \tag{3.57}$$

$$\Omega^2_{L/R,11} = k^2 - a^2H^2\frac{(1-\delta)^2(2+\epsilon_Q)+\gamma(2-3\epsilon_Q)}{(1-\delta)^2+\gamma}, \tag{3.58}$$

$$\begin{aligned}\Omega^2_{L/R,12} = \pm aHk\frac{2\sqrt{\gamma\epsilon_Q}}{\sqrt{(1-\delta)^2+\gamma}} - a^2H^2\frac{\sqrt{\epsilon_Q}}{\sqrt{(1-\delta)^2+\gamma}}\cdot \\ \cdot\Bigg[\frac{(2\gamma^2+3\gamma(1-\delta))(2-\Upsilon-(\epsilon_Q+2/3\epsilon_\varphi))+}{(2-\Upsilon-2/3\epsilon_\varphi)(1-\delta)^2+\gamma(2-\Upsilon-(\epsilon_Q+2/3\epsilon_\varphi))}+ \\ +\frac{(1-\delta)^3(2-\Upsilon-2\epsilon_Q-2/3\epsilon_\varphi+2\delta(2-\Upsilon-(\epsilon_Q+2/3\epsilon_\varphi)))}{(2-\Upsilon-2/3\epsilon_\varphi)(1-\delta)^2+\gamma(2-\Upsilon-(\epsilon_Q+2/3\epsilon_\varphi))}\Bigg],\end{aligned} \tag{3.59}$$

$$\begin{aligned}\Omega^2_{L/R,22} = k^2 \mp 2aHk\frac{1}{\sqrt{\gamma}}\cdot \\ \cdot\Bigg[\frac{(2\gamma^2+(1-\delta)^3(1+\delta))(2-\Upsilon-(\epsilon_Q+2/3\epsilon_\varphi))}{(2-\Upsilon-2/3\epsilon_\varphi)(1-\delta)^2+\gamma(2-\Upsilon-(\epsilon_Q+2/3\epsilon_\varphi))}+ \\ +\frac{\gamma(1-\delta)(3(2-\Upsilon)-\delta(2-\Upsilon-2/3\epsilon_\varphi)-2\epsilon)}{(2-\Upsilon-2/3\epsilon_\varphi)(1-\delta)^2+\gamma(2-\Upsilon-(\epsilon_Q+2/3\epsilon_\varphi))}\Bigg]+ \\ +2a^2H^2\frac{(2-\Upsilon-(\epsilon_Q+2/3\epsilon_\varphi))(\gamma^2+2(1-\delta)\gamma+(1+\delta)(1-\delta)^3)}{(2-\Upsilon-2/3\epsilon_\varphi)(1-\delta)^2+\gamma(2-\Upsilon-(\epsilon_Q+2/3\epsilon_\varphi))}.\end{aligned} \tag{3.60}$$

Now, we substitute ϵ_Q and δ from Eq. (3.22), i.e.

$$\epsilon_Q \to \epsilon - \epsilon_\varphi \quad , \quad \delta \to \frac{\epsilon}{3(2-\Upsilon-(\epsilon-\frac{1}{3}\epsilon_\varphi))}\left(\epsilon - \frac{2}{3}\frac{\epsilon_\varphi}{\epsilon}\eta_\varphi - \frac{\epsilon_\varphi}{3} + \Upsilon\left(1-\frac{\epsilon_\varphi}{\epsilon}\right)\right) \tag{3.61}$$

and expand the matrix elements in slow roll with $\epsilon \ll 1$ and $\epsilon_\varphi \ll 1$. The lowest order in slow-roll quantities is $\sqrt{\epsilon}$, where we obtain

$$K_{L/R,12} \simeq aH\frac{\sqrt{\epsilon}}{\sqrt{1+\gamma}}\,C_1(\epsilon_\varphi), \tag{3.62}$$

$$\Omega^2_{L/R,11} \simeq k^2 - 2a^2H^2, \tag{3.63}$$

$$\Omega^2_{L/R,12} \simeq \left(\pm 2kaH\frac{\sqrt{\gamma\epsilon}}{\sqrt{1+\gamma}} - a^2H^2\frac{1+2\gamma}{\sqrt{1+\gamma}}\sqrt{\epsilon}\right)C_1(\epsilon_\varphi), \tag{3.64}$$

$$\Omega^2_{L/R,22} \simeq k^2 \mp 2kaH\frac{1}{\sqrt{\gamma}}\left[1+2\gamma+C_2(\epsilon_\varphi)\right] + 2a^2H^2\left[1+\gamma+C_2(\epsilon_\varphi)\right], \tag{3.65}$$

where we introduced the "correction" coefficients

$$C_1(\epsilon_\varphi) = \sqrt{1 - \frac{\epsilon_\varphi}{\epsilon}}, \tag{3.66}$$

$$C_2(\epsilon_\varphi) = -\frac{\epsilon}{2-\Upsilon}\left(1 - \frac{\epsilon_\varphi}{\epsilon}\right) + \mathcal{O}(\epsilon). \tag{3.67}$$

Notice that when the inflaton field dominates the energy budget, Eq. (3.10) leads to $\Upsilon \sim 2$. Hence the second correction can be $\frac{\epsilon}{2-\Upsilon}\left(1 - \frac{\epsilon_\varphi}{\epsilon}\right) \sim \sqrt{\epsilon}$ and is not negligible any more. For the case $\epsilon_\varphi = 0$ and $\Upsilon = 0$, matrix elements reduce to the case of pure Gauge-flation and agree with the results obtained in Ref. [233]. The absolute value of the corrections $C_1(\epsilon_\varphi)$ and $C_2(\epsilon_\varphi)$ depend on the fraction of energy stored in the inflaton field, i.e. $\epsilon_\varphi/\epsilon$. There is an interesting "tug of war" between two different effects here.

- Since $1 - \epsilon_\varphi/\epsilon = \epsilon_Q/\epsilon$, GW production by the gauge sector requires $\epsilon_\varphi/\epsilon$ to deviate somewhat from unity.

- The requirement that the gauge-sector does not affect the dynamics of inflation and the generation of density fluctuations is encoded in $\epsilon_\varphi \gg \epsilon_Q$ or $\epsilon_Q/\epsilon \ll 1$.

Both requirements, the dominance of the inflaton sector and significant GW production by the gauge sector, can be simultaneously satisfied, but limit the available parameter space.

The equation of motion for tensor perturbations follows from Eq. (3.50) and may be written in the form

$$\Delta_L'' + 2K_L\Delta_L' + (K_L' + \Omega_L^2)\Delta_L = 0, \tag{3.68}$$

and similarly for the right-handed sector. To leading order in $\sqrt{\epsilon}$ and neglecting interactions with the gravitational wave sector, the equation of motion for the gauge field perturbation reads

$$\partial_\tau^2 T_L + \Omega_{L,22}^2 T_L = 0. \tag{3.69}$$

Substituting the matrix $\Omega_{L,22}^2$ explicitly with $\tau = -\frac{1}{aH}$ we get

$$\partial_\tau^2 T_L + \left(k^2 - \frac{2k}{-\tau}\frac{1 + 2\gamma + C_2(\epsilon_\varphi)}{\sqrt{\gamma}} + \frac{2\left(1 + \gamma + C_2(\epsilon_\varphi)\right)}{\tau^2}\right) T_L = 0. \tag{3.70}$$

Now, we may define $z = 2ik\tau$ and

$$\hat{\nu} = \frac{2\left(1 + 2\gamma + C_2(\epsilon_\varphi)\right)}{\sqrt{\gamma}} = -2i\hat{\alpha}, \tag{3.71}$$

$$\hat{\mu} = 2\left(1 + \gamma + C_2(\epsilon_\varphi)\right) = \frac{1}{4} - \hat{\beta}^2, \tag{3.72}$$

in order to rewrite Eq. (3.70) in the form of the Whittaker equation

$$\partial_z^2 T_L + \left(-\frac{1}{4} + \frac{\hat{\alpha}}{z} + \frac{\frac{1}{4} - \hat{\beta}^2}{z^2}\right) T_L = 0. \tag{3.73}$$

It can be solved with the Whittaker functions

$$T_{L,0}(k,\tau) = A_k M_{\hat{\alpha},\hat{\beta}}(2ik\tau) + B_k W_{\hat{\alpha},\hat{\beta}}(2ik\tau), \tag{3.74}$$

with $M_{\hat{\alpha},\hat{\beta}}(2ik\tau)$ and $W_{\hat{\alpha},\hat{\beta}}(2ik\tau)$ being the Whittaker M and W functions. Here the subscript 0 indicates that we neglected interactions with the gravitational wave sector. In the asymptotic past $x \equiv -k\tau \to \infty$, the solution approaches the Bunch-Davies vacuum, i.e.

$$T_{L,0}(k,\tau) \to \frac{1}{\sqrt{2k}} e^{ix}. \tag{3.75}$$

Asymptotic expansions for the Whittaker functions in this limit are also well-known, hence the constants A_k and B_k in (3.74) are given by [232]

$$A_k = \frac{1}{\sqrt{2k}} \frac{\Gamma\left(-\hat{\alpha} + \hat{\beta} + \frac{1}{2}\right)}{(2i)^{-\hat{\alpha}}\Gamma\left(2\hat{\beta} + 1\right)}, \tag{3.76}$$

$$B_k = \frac{1}{\sqrt{2k}} \frac{\Gamma\left(-\hat{\alpha} + \hat{\beta} + \frac{1}{2}\right)}{\Gamma\left(\hat{\alpha} + \hat{\beta} + \frac{1}{2}\right)} 2^{\hat{\alpha}} i^{\hat{\beta}+1} (-i)^{\hat{\alpha}-\hat{\beta}}. \tag{3.77}$$

Next, we find that metric tensor modes to leading order in $\sqrt{\epsilon}$ satisfy the following equation of motion in the x-variable

$$\partial_x^2 H_L + \left(1 - \frac{2}{x^2}\right) H_L = \frac{\sqrt{\epsilon}\, C_1(\epsilon_\varphi)}{\sqrt{1+\gamma}} \left(\frac{2}{x}\partial_x T_L + \left(\frac{2\gamma}{x^2} - \frac{2\sqrt{\gamma}}{x}\right) T_L\right). \tag{3.78}$$

Using the Born approximation, one may find the solution of Eq. (3.78) in series of $\sqrt{\epsilon}$

$$H_L = H_{L,0} + H_{L,s}, \tag{3.79}$$

where $H_{L,0}$ is the homogeneous solution of the free equation of motion, and $H_{L,\mathrm{s}}$ is inhomogeneous part that is sourced by the gauge filed perturbation T_L. The homogeneous solution matches the Bunch-Davies vacuum at asymptotic past and is given by

$$H_{L,0} = \frac{1}{\sqrt{2k}}\left(1+\frac{i}{x}\right)e^{ix}. \tag{3.80}$$

The sourced piece of the solution may be written as

$$H_{L,s} = \frac{\sqrt{\epsilon}\,C_1(\epsilon_\varphi)}{\sqrt{1+\gamma}}\int^x dx'\left(\frac{2}{x'}\partial_{x'}+\left(\frac{2\gamma}{x'^2}-\frac{2\sqrt{\gamma}}{x'}\right)\right)G(x,x')T_{L,0}(x'), \tag{3.81}$$

where $G(x,x')$ is the Green's function. We can follow the same steps as in Refs. [229, 231, 232] and find that the late-time solution for the left-handed gravitational wave is given by

$$H_L = \frac{Hx}{M_{\rm Pl}\sqrt{k^3}}u_1(x)+2\sqrt{2}\frac{H}{M_{\rm Pl}k}B_k\frac{2\sqrt{\epsilon}\,C_1(\epsilon_\varphi)}{\sqrt{1+\gamma}}\left(I_1+\sqrt{\gamma}I_2-\gamma I_3\right), \tag{3.82}$$

which contains a free and a sourced part of the solution. Here we have defined

$$u_1(x) \equiv \left(1+\frac{i}{x}\right)e^{ix}. \tag{3.83}$$

The terms I_1, I_2, I_3 are coming from the integrals in Eq. (3.81) and expressed as

$$I_1 = \frac{\left(\hat{\mu}^2-2i\hat{\mu}\hat{\nu}+2\hat{\mu}-2\hat{\nu}^2\right)\sec(\pi\hat{\beta})\sinh(-i\pi\hat{\alpha})\Gamma(\hat{\alpha})}{2\hat{\mu}(\hat{\mu}+2)} \tag{3.84}$$

$$-\frac{\pi^2\left(\hat{\mu}^2+2i\hat{\mu}\hat{\nu}+2\hat{\mu}-2\hat{\nu}^2\right)\sec(\pi\hat{\beta})\mathrm{csch}(-i\pi\hat{\alpha})}{2\hat{\mu}(\hat{\mu}+2)\Gamma(\hat{\alpha}+1)\Gamma(-\hat{\alpha}-\hat{\beta}+\frac{1}{2})\Gamma(-\hat{\alpha}+\hat{\beta}+\frac{1}{2})}, \tag{3.85}$$

$$I_2 = \frac{\pi\sec(\pi\hat{\beta})\Gamma(-\hat{\alpha})}{2\Gamma(-\hat{\alpha}-\hat{\beta}+\frac{1}{2})\Gamma(-\hat{\alpha}+\hat{\beta}+\frac{1}{2})}-\frac{\pi\sec(\pi\hat{\beta})\Gamma(1-\hat{\alpha})}{\hat{\mu}\Gamma(-\hat{\alpha}-\hat{\beta}+\frac{1}{2})\Gamma(-\hat{\alpha}+\hat{\beta}+\frac{1}{2})}$$
$$+\frac{\pi\hat{\mu}\sec(\pi\hat{\beta})-i\pi\hat{\nu}\sec(\pi\hat{\beta})}{2\hat{\mu}\Gamma(1-\hat{\alpha})}, \tag{3.86}$$

$$I_3 = \frac{\pi^2\left(\hat{\mu}+i\hat{\nu}\right)\sec(\pi\hat{\beta})\mathrm{csch}(-i\pi\hat{\alpha})}{\hat{\mu}(\hat{\mu}+2)\Gamma(\hat{\alpha})\Gamma(-\hat{\alpha}-\hat{\beta}+\frac{1}{2})\Gamma(-\hat{\alpha}+\hat{\beta}+\frac{1}{2})}+\frac{\pi\left(\hat{\nu}+i\hat{\mu}\right)\sec(\pi\hat{\beta})}{\hat{\mu}(\hat{\mu}+2)\Gamma(-\hat{\alpha})}. \tag{3.87}$$

The homogeneous solution for the gauge field perturbation $T_{L,0}$ is an excellent approximation, since it breaks down for $x \lesssim 0.1$, which does not influence gravitational wave modes which are sourced around horizon crossing $x \simeq 1$. Indeed, we see that the late-time solution of Eq. (3.82) is in a remarkable agreement with full numerical simulations, as seen on Fig. 3.6.

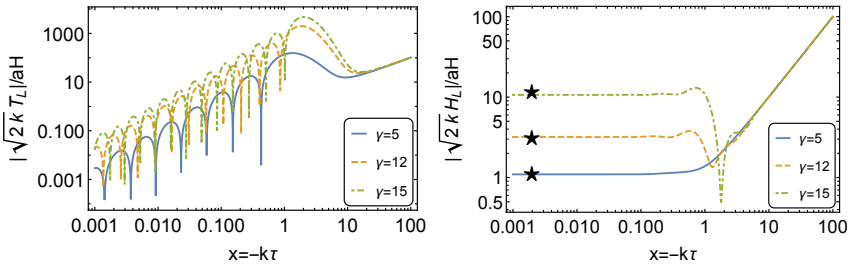

Figure 3.6: *Left:* Tachyonic growth of the left-polarized gauge field mode-function T_L around the time of horizon crossing $x = 1$ for $\gamma = 5, 12, 15$ (blue solid, orange dashed and green dot-dashed lines respectively), $H/M_{\rm pl} = 1.9{*}10^{-6}$ and $g = 6.5{*}10^{-3}$. *Right:* Enhancement of the left-polarized GW mode-function H_L, sourced by the gauge field mode-function T_L for the same parameters and color coding. Stars represent the approximate late-time solutions given by Eq. (3.82).

The right-hand polarized gravitational waves do not get enhanced and are given by the usual vacuum value

$$H_R(x) = \frac{Hx}{M_{\rm Pl}\sqrt{k^3}} u_1(x). \tag{3.88}$$

Finally, the power spectra for left-handed modes can be written as

$$P_L^2(k) = \frac{H^2}{2\pi^2 M_{\rm Pl}^2} + \frac{16kH^2}{\pi^2 M_{\rm Pl}^2} \frac{\epsilon\, C_1^2(\epsilon_\varphi)}{1+\gamma} |B_k|^2 \left|I_1 + \sqrt{\gamma} I_2 - \gamma I_3\right|^2 . \tag{3.89}$$

The power spectra for right-handed modes is

$$P_R^2(k) = \frac{H^2}{2\pi^2 M_{\rm Pl}^2}. \tag{3.90}$$

The total tensor power spectrum is given by

$$P_T(k) = 2P_L^2(k) + 2P_R^2(k), \tag{3.91}$$

which in the limit $\epsilon \to \epsilon_\varphi$, i.e. $C_1(\epsilon_\varphi) \to 0$, reduces to the single scalar field result

$$P_{T,\varphi}(k) = \frac{2H^2}{\pi^2 M_{\rm Pl}^2}, \tag{3.92}$$

Finally, we can define the chirality parameter as

$$\Delta\chi = \frac{P_L^2 - P_R^2}{P_L^2 + P_R^2}. \tag{3.93}$$

Its behaviour is shown on Fig. 3.7. We see that sufficient enhancement of

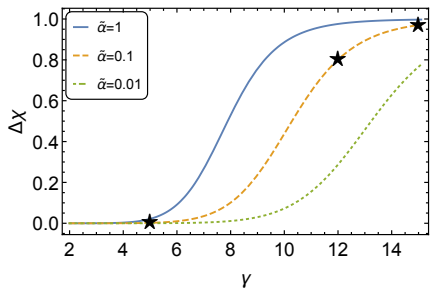

Figure 3.7: The chirality parameter $\Delta\chi$ as a function of γ for $\tilde{\alpha} = 1, 0.1, 0.01$ (blue solid, orange dashed and green dot-dashed lines respectively) for $H/M_{\rm pl} = 1.9 * 10^{-6}$, $g = 6.5 * 10^{-3}$. Stars represent $\gamma = 5, 12, 15$ used in Fig. (3.6).

one of the polarizations occurs for $\gamma \gtrsim 8$ for the given set of parameters ($H = 1.9 \times 10^{-6} M_{\rm pl}$, $\epsilon = 10^{-5}$, $g = 6.5 \times 10^{-3}$). For these parameters $\gamma_{\rm max} \simeq 15$.

3.4.2 Tensor tilt

In this subsection we will discuss the shape of the tensor power spectrum generated in the spectator Gauge-flation model, characterized by the tensor tilt n_T. In Ref. [239], it was shown that the spectator Chromo-natural inflation model, depending on the choice of the axion potential, supports both flat, red and blue tilted tensor spectra. Thus, our primary interest is to investigate if spectator Gauge-flation may generate all three possible tilts in realistic physical set-ups. The tensor tilt for Eq. (3.92) is given by $n_T = -2\epsilon_*$, where ϵ is evaluated at $t = t_*$ that defines time of horizon crossing for a mode with the wave number $k_* = a(t_*)H$. Below we will focus on the tilt for the sourced part only.

The power spectra of sourced gravitational waves from Eqs. (3.89) and (3.91) are given by

$$P_{T,s}(k) = \frac{32kH^2}{\pi^2 M_{\rm Pl}^2} \frac{\epsilon\, C_1^2(\epsilon_\varphi)}{1+\gamma} |B_k|^2 \left|I_1 + \sqrt{\gamma} I_2 - \gamma I_3\right|^2. \tag{3.94}$$

We are going to proceed as follows: first we rewrite Eq. (3.94) in terms of $\gamma(t)$, restoring its time-dependence, and then re-express $P^2_{T,s}(k)$ in terms of $\gamma(k)$. This allows us to calculate the tensor tilt.

The time evolution of the vacuum expectation value of the gauge field $Q(t)$ may be written as

$$Q(t) = Q(t_*) + \dot{Q}(t_*)(t - t_*), \tag{3.95}$$

with t_* being the time of horizon crossing. From here it follows that

$$\frac{Q(t)}{Q(t_*)} = 1 - \delta_* H(t - t_*), \tag{3.96}$$

where $\delta_* = -\frac{\dot{Q}(t_*)}{HQ(t_*)}$. This gives the time dependence of the parameter $\gamma(t)$, i.e.

$$\gamma(t) = \gamma_* \left(\frac{Q(t)}{Q(t_*)}\right)^2 = \gamma_* \left(1 - \delta_* H(t - t_*)\right)^2 \simeq \gamma_* \left(1 + 2\frac{H(t - t_*)}{\Delta N}\right), \tag{3.97}$$

with $\gamma_* = \frac{g^2 Q^2(t_*)}{H^2}$, $\Delta N = -1/\delta_*$. Using $H(t - t_*) = \ln(k/k_*)$ we can write $\gamma(k)$ as

$$\gamma(k) \simeq \gamma_* \left(1 + 2\frac{\ln(k/k_*)}{\Delta N}\right) \simeq \gamma_* e^{\left(\frac{2\ln(k/k_*)}{\Delta N}\right)}. \tag{3.98}$$

To start with, using $|\Gamma(\frac{1}{2} + ib)|^2 = \frac{\pi}{\cosh(\pi b)}$ one can rewrite $|B_k|^2$ defined in Eq. (3.76) in terms of $\gamma(t)$ as

$$|B_k|^2 = \frac{1}{2k} e^{3\pi\left(\frac{1+2\gamma}{\sqrt{\gamma}}\right)} e^{-\pi\sqrt{7+8\gamma}} \frac{1 + e^{-\pi\left(\sqrt{7+8\gamma} + \frac{2(1+2\gamma)}{\sqrt{\gamma}}\right)}}{1 + e^{-\pi\left(\sqrt{7+8\gamma} - \frac{2(1+2\gamma)}{\sqrt{\gamma}}\right)}}. \tag{3.99}$$

Next, from Eq. (3.17) for $\delta \ll 1$ one can find

$$\epsilon\, C_1^2(\epsilon_\varphi) = \epsilon_Q \simeq \frac{H^2}{g^2 M_{\rm Pl}^2} \gamma(1 + \gamma). \tag{3.100}$$

The term γI_3 generates the main contribution in Eq. (3.94), hence we will neglect smaller contributions coming from $I_1, \sqrt{\gamma} I_2$. In terms of γ we find

$$\gamma^2 |I_3|^2 = \gamma^2 \frac{\pi\,(1 + 2\gamma)(1 + \gamma(1 + \gamma)(5 + \gamma))}{\gamma^{3/2}(1 + \gamma)^2(2 + \gamma)^2} e^{-\pi\left(\sqrt{7+8\gamma} - \frac{1+2\gamma}{\sqrt{\gamma}}\right)}. \tag{3.101}$$

Putting everything together, the sourced tensor power spectrum becomes

$$P_{T,s}(k) \simeq \frac{16H^4}{\pi^2 g^2 M_{\rm Pl}^4}\gamma\, e^{3\pi\left(\frac{1+2\gamma}{\sqrt{\gamma}}\right)} e^{-\pi\sqrt{7+8\gamma}}\, \frac{1+e^{-\pi\left(\sqrt{7+8\gamma}+\frac{2(1+2\gamma)}{\sqrt{\gamma}}\right)}}{1+e^{-\pi\left(\sqrt{7+8\gamma}-\frac{2(1+2\gamma)}{\sqrt{\gamma}}\right)}}\, |\gamma I_3|^2\,, \tag{3.102}$$

where $|\gamma I_3|^2$ is given by Eq. (3.101). Next, one may expand

$$\sqrt{7+8\gamma} = \sqrt{7+8\gamma_*} + \frac{8\gamma_*}{\sqrt{7+8\gamma_*}\Delta N}\ln\left(\frac{k}{k_*}\right) - \frac{32\gamma_*^2}{(7+8\gamma_*)^{3/2}(\Delta N)^2}\ln^2\left(\frac{k}{k_*}\right), \tag{3.103}$$

$$\frac{1+2\gamma}{\sqrt{\gamma}} = \frac{1+2\gamma_*}{\sqrt{\gamma_*}} + \frac{2\gamma_*-1}{\sqrt{\gamma_*}\Delta N}\ln\left(\frac{k}{k_*}\right) - \frac{\gamma_*-3/2}{\sqrt{\gamma_*}(\Delta N)^2}\ln^2\left(\frac{k}{k_*}\right). \tag{3.104}$$

We will not write the final expression for $P_{T,s}(k)$ in terms of γ_*, k, k_* since it is rather cumbersome, but may be easily written from the above expressions. Instead, we will focus on the tensor tilt. As usual, the tensor power spectra may be written in the form

$$P_{T,s}(k) = A_T(\gamma_*)\left(\frac{k}{k_*}\right)^{n_{T,s}}, \tag{3.105}$$

with the tensor tilt is given by

$$\begin{aligned} n_{T,s} = \frac{d\ln P_{T,s}(k)}{d\ln k} = &-\delta_*\,[3 + 4\pi\frac{2\gamma_*-1}{\sqrt{\gamma_*}} - 16\pi\frac{\gamma_*}{\sqrt{7+8\gamma_*}} \\ &- \frac{2\gamma_*(-8-39\gamma_*-57\gamma_*^2-23\gamma_*^3+\gamma_*^4)}{(1+\gamma_*)(2+\gamma_*)(1+2\gamma_*)(1+5\gamma_*+6\gamma_*^2+\gamma_*^3)} \\ &- \pi\frac{\frac{8\gamma_*}{\sqrt{7+8\gamma_*}} + 2\frac{2\gamma_*-1}{\sqrt{\gamma_*}}}{1+e^{\pi\left(\sqrt{7+8\gamma_*}+2\frac{1+2\gamma_*}{\sqrt{\gamma_*}}\right)}} + \pi\frac{\frac{8\gamma_*}{\sqrt{7+8\gamma_*}} - 2\frac{2\gamma_*-1}{\sqrt{\gamma_*}}}{1+e^{\pi\left(\sqrt{7+8\gamma_*}-2\frac{1+2\gamma_*}{\sqrt{\gamma_*}}\right)}}], \end{aligned} \tag{3.106}$$

where we neglected corrections $\mathcal{O}\left(\delta_*^2\right)$ and ignored the time-dependence of H. For α-attractors, as well as other plateau models, this is a very good approximation. The complicated expression above may be written via a simple fitting formula

$$n_{T,s} \simeq -\delta_*\left(3 + 1.225\pi\frac{2\gamma_*-1}{\sqrt{\gamma_*}} - 3.612\pi\frac{\gamma_*}{\sqrt{7+8\gamma_*}}\right) \simeq -\delta_*\left(2.85 + 3.68\sqrt{\gamma_*}\right). \tag{3.107}$$

Hence, we may conclude that if $Q(t)$ is a decreasing function of time, then $\delta(t)$ defined in Eq. (3.16) leads to δ_* being positive. Therefore, as follows from Eq. (3.107), a red-tilted power spectrum is generated. If, on the contrary, $Q(t)$ increases in time, $\delta(t)$ is negative, which sources a blue-tilted spectrum. We can sum up the relation of $Q(t)$ to n_T in the following table

$$\begin{array}{lllllll} Q(t)\searrow & \Rightarrow & \dot{Q}(t)<0 & \Rightarrow & \delta>0 & \Rightarrow & n_T<0 \quad \text{red tilt,} \\ Q(t)\nearrow & \Rightarrow & \dot{Q}(t)>0 & \Rightarrow & \delta<0 & \Rightarrow & n_T>0 \quad \text{blue tilt.} \end{array} \tag{3.108}$$

All the results shown in Section 3.3 contain $Q(t)$ as a decreasing function of time, leading to red-tilted tensor spectra. Finally, Eq. (3.91) leads to the tensor-to-scalar ratio r

$$r = \frac{P_T}{P_\zeta}. \tag{3.109}$$

The left panel of Fig. 3.8 shows the enhancement of the tensor-to-scalar ratio r and its dependence on γ for the α-attractor potential of Eq. (3.41) with $n = 3/2$ and $\tilde{\alpha} = 10, 1, 0.1, 0.01$. We see that for small γ, we recover the single field α-attractor result $r = 16\epsilon$ with $\epsilon \to \epsilon_\varphi \simeq \frac{3\tilde{\alpha}}{4N^2}$. Further increasing r requires decreasing the gauge coupling g. However this is severely restricted by Eqs. (3.28) and (3.45), meaning that we cannot increase r significantly above what is show on Fig. 3.8. The right panel of Fig. 3.8 shows the correlation of Eq. (3.107) and r using Eq. (3.22). We see that $0 > n_T \gtrsim -0.04$ and larger r correlates with more red-tilted spectra.

Before we proceed to a brief overview of related models and comparison with our results on spectator gauge-flation, it is worth discussing the conditions for a red-tilted spectrum. It was shown in Ref. [76] that the original gauge-flation model can lead (at the background level) to both decreasing and growing functions of $Q(t)$, depending on the initial conditions. Trajectories starting close to the slow-roll attractor lead to a decreasing $Q(t)$. Trajectories that start far from the slow roll attractor in Ref. [76] were shown to undergo a brief period of $\epsilon > 1$, followed by a slow-roll inflationary phase with $Q(t)$ increasing in time. The latter behavior required different ranges of κ and g.

We were able to recover this general trend in our spectator model, at the cost of altering the parameter space of the model. In particular, to produce a growing $Q(t)$ and a correspondingly blue-tilted GW spectrum, we need to increase the value of κ. This leads to an increase in ρ_κ, which is bounded from above by the requirement $\rho_\kappa \ll \rho_\varphi$. Furthermore, γ is reduced for these trajectories, suppressing GW production by the spectator

sector. In order to increase GW production, we need to increase g, which cannot be done arbitrarily. Such a realization of spectator gauge-flation is given in Appendix 3A. Our numerical tests have shown the existence of such solutions, but at the same time an increased level of parameter fine-tuning is needed to achieve them, at least in the context of an α-attractor inflationary sector. We will consider the red-tilted GW spectra as a "generic" prediction of spectator gauge-flation, keeping in mind the ability of these models to evade this prediction for proper choices of parameters and initial conditions. We leave an exhaustive parameter search for a variety of inflationary sectors for future work.

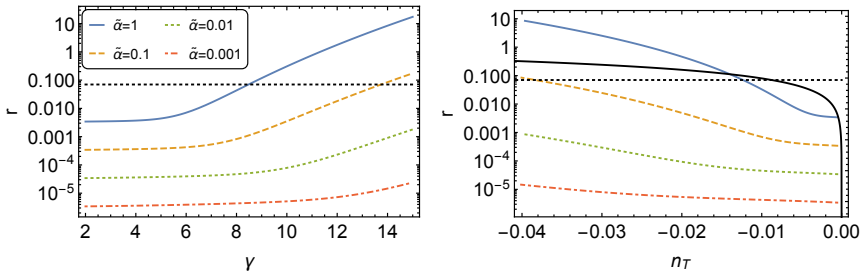

Figure 3.8: *Left:* The tensor-to-scalar ratio r as a function of γ for $g = 6.5 \times 10^{-3}$ and $\tilde{\alpha} = 1, 0.1, 0.01, 0.001$ (blue solid, orange dashed, green dotted and red dot-dashed lines respectively). The horizontal black-dotted curve shows the observational upper limit on r. *Right:* The tensor-to-scalar ratio r versus tensor tilt n_T for the same parameters and color coding. We can see the range of n_T and the clear departure from the single field consistency relation $n_T = -r/8$ (solid black curve).

3.4.3 Comparison with related models

The model presented here is part of a larger family of inflationary models, where the existence of a non-abelian sector leads to the generation of chiral GWs. We can distinguish between the original models, where the $SU(2)$ or axion$-SU(2)$ sectors are responsible for inflation and the generation of both scalar and tensor modes, and the spectator models, where the inflaton sector is decoupled from the non-abelian spectator sector. Gauge-flation and Chromo-natural inflation, along with their Higgsed variants, fit in the first category, while spectator Chromo-natural inflation and spectator Gauge-flation make up the second category.

While the original Chromo-natural inflation and Gauge-flation models are ruled out by observations, their Higgsed counterparts provide predictions compatible with CMB observations for some part of parameter

space. Interesting features arise from the correlation of the resulting tensor to scalar ratio r and tensor spectral tilt n_T. For Higgsed gauge-flation, Ref. [232] showed a negative correlation between the two quantities. For $n \lesssim 0.01$ a blue-tilted spectrum is preferred. Hence Higgsed gauge-flation and spectator gauge-flation (with an α-attractor inflationary sector) tend to provide opposite predictions for the sign of n_T.

Higgsed chromo-natural inflation has an interesting space of predictions for n_T and r. For smaller values of $r < 0.01$, the correlation between r and n_T is also mostly negative. However the possible range of values for n_T is much larger, ranging between $-0.2 < n_T < 0.05$ for the parameter scan presented in Ref. [231]. This means that the possible range of values for Higgs Chromo-Natural inflation is significantly larger than that of our realization of spectator Gauge-flation (see Fig. 3.8) for red and blue tilted spectra alike.

Next, we wish to compare the present model to spectator Chromo-natural inflation, in which an axion$-SU(2)$ spectator sector is added to an otherwise dominant inflaton. The existence of an axion potential $V(\chi)$ leads for significant diversity in the form of the tensor power spectrum. Ref. [239] showed the emergence of a blue or red-tilted spectrum for monomial potential $V(\chi) \propto |\chi|^p$, where the tensor tilt scales as $n_T \propto (p-1)$. A linear potential leads to an exactly scale-invariant tensor spectrum. In principle, small deviations from $p = 1$ can lead to an arbitrarily small tensor tilt. However, this requires a rather fine-tuned axion potential. If instead we look at $p = 1/2$ and $p = 3/2$ we can see that $n_T \simeq 0.04$ and $n_T \simeq -0.07$ respectively. Concave potentials lead to blue-tilted spectra, which are generically not produced in our model of spectator Gauge-flation. On the other hand, convex potentials lead to red-tilted spectra, but for $p > 3/2$ the spectral tilt will be $n_T \lesssim \mathcal{O}(0.1)$, which is outside the predictions shown in Fig. 3.8.

Finally, Ref. [246] studied an axion-inflaton field coupled to an $SU(2)$ gauge field, where the VEV of the latter is not large enough to affect the background inflationary dynamics. Despite being subdominant, the presence of the gauge field can lead to the enhancement of GW's and the corresponding violation of the Lyth bound. The resulting tensor tilt n_T exhibits oscillations in time and asymptotes to zero at late times.

3.5 Summary and discussion

In this work we have explored the phenomenology of Gauge-flation as a spectator sector during inflation. We have uncovered significant parameter

restrictions, arising both from the physics of the gauge sector as well as from the requirements that the gauge sector be subdominant to the inflationary sector. Most importantly, these requirements lead to significant constraints on the parameter γ, which controls the amount of GW enhancement.

By identifying the inflationary sector with the well-known T-model of α-attractors, we showed that a spectator gauge-flation sector can increase the tensor-to-scalar ratio by two orders of magnitude. The resulting tensor spectral index n_T is controlled by the evolution of the gauge field vacuum expectation value $Q(t)$, being red if Q is a decreasing function of time during inflation and blue otherwise. The majority of our numerical simulations resulted in red-tilted GW spectra with $-0.04 \lesssim n_T < 0$.

Our work presents an interesting generalization of gauge-flation, while opening up exciting possibilities for future work. While α-attractors provide a simple implementation of the inflationary sector, inflationary models that contain two or more distinct phases of inflation, like double inflation, side-tracked inflation and angular inflation, can help alleviate the parameter constraints of our current implementation and produce distinct GW features either at large or small scales. Furthermore, inflationary models with non-Abelian gauge fields can have interesting consequences for baryogenesis and dark matter production [247–250], leading to correlated observables.

Furthermore, the original choice of the higher-order term for gauge-flation was based on the requirement for a vacuum energy-like equation of state $w \simeq -1$, required for driving inflation. Using an $SU(2)$ sector as a spectator sector opens up the possibility of introducing more non-linear terms, since the requirement of $w \simeq -1$ is lifted. It is interesting to explore the phenomenology of gauge-flation with other non-linear terms, dictated solely by the underlying symmetries, and their possible GW signatures. We leave this exploration for future work.

3.6 Appendix 3A: Blue-tilted GW spectrum

As shown in Eq. (3.108), the dynamics of $Q(t)$ controls the sign of the tensor tilt n_T. Here we present a realization where $Q(t)$ is an increasing function of time on the example of α-attractor model, similarly as in Section 3.3, for the same parameters of Eq. (3.42) for the potential, but with $\tilde{\alpha} = 1$. The parameters we use for the gauge sector are

$$\begin{aligned} g = 1.7 \times 10^{-2}, \quad \kappa = 10^{21}\, M_{\rm pl}^{-4}, \\ \dot{Q}_0/M_{\rm pl}^2 = 10^{-10}, \quad Q_0/M_{\rm pl} = 6 \times 10^{-4}, 8 \times 10^{-4}, 1.18 \times 10^{-3}. \end{aligned} \tag{3.110}$$

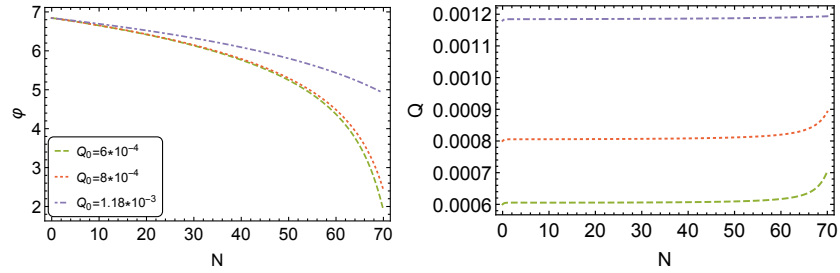

Figure 3.9: *Left:* The dependence of the inflaton field φ on the e-folding number N for the the α-attractor T-model potential of Eq. (3.41) for $Q_0/M_{\rm pl} = 6\times10^{-4}, 8\times10^{-4}, 1.18\times10^{-3}$ (green-dashed, red-dotted and purple-dot-dashed lines respectively). *Right:* The dependence of the gauge field VEV Q on the e-folding number N for the same potential and color coding.

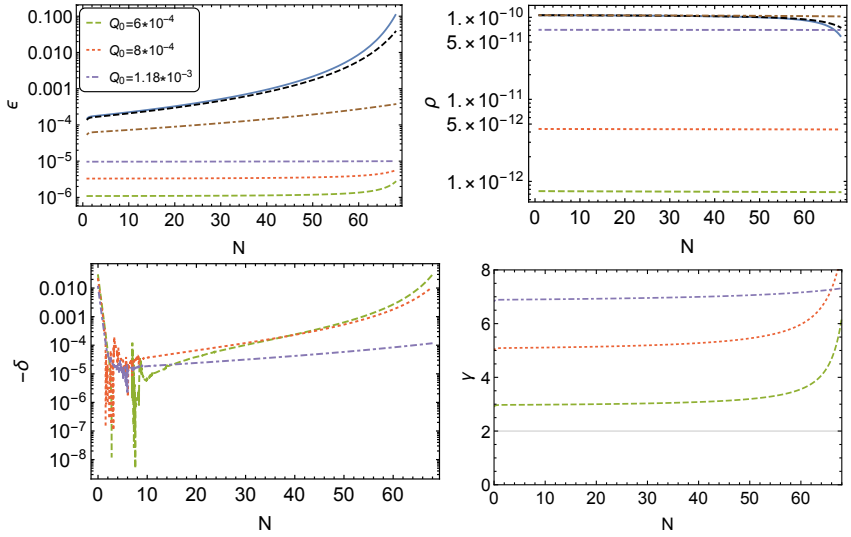

Figure 3.10: *Top left:* Components ϵ_{Q_B} as a function of the e-folding number N for $Q_0/M_{\rm pl} = 6\times10^{-4}, 8\times10^{-4}, 1.18\times10^{-3}$ (green-dashed, red-dotted and purple-dot-dashed lines respectively). The blue-solid, black-dashed and brown-dot-dashed and curved correspond to ϵ_φ for $Q_0/M_{\rm pl} = 6\times10^{-4}, 8\times10^{-4}, 1.18\times10^{-3}$ respectively. *Top right:* Components ρ_κ and their dependence on N for the same Q_0 and color-coding. The very top curves correspond to ρ_φ and are practically indistinguishable. *Bottom row:* The evolution of the parameter δ (left) and γ (right) for the same parameters and color-coding. The solid grey grid line on the right panel shows the bound $\gamma = 2$, below which scalar fluctuations in the theory are unstable.

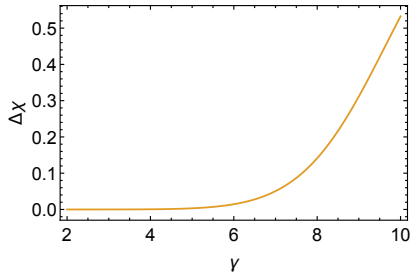

Figure 3.11: The chirality parameter $\Delta\chi$ as a function of γ for $\tilde{\alpha} = 1$, $H/M_{\rm pl} = 6 * 10^{-6}$ and $g = 1.7 * 10^{-2}$. In the allowed region $\gamma \lesssim 7$, the chirality parameter is small.

Our numerical simulations show that in order for $Q(t)$ to increase with time, one has to impose higher values of the parameter κ in comparison with those used in Section 3.3. Because of the conditions of Eqs. (3.33) and (3.39), this highly constrains the values of the allowed Q_0 and g, and hence via Eq. (3.16) limits the allowed range for the parameter γ that controls the enhancement of chiral gravitational waves.

Fig. 3.9 shows the evolution of the inflaton field φ and the vacuum expectation value of the gauge field Q with the e-folding number N, that behave similarly to those discussed in Section 3.3, but with Q being a slowly increasing function of time. In such case δ becomes negative, as shown in Fig. 3.10. However, one may see from the top right panel of the Fig. 3.10, that further increase of Q_0 will violate the condition $\rho_\varphi \gg \rho_{Q_\kappa}$. Hence for the parameters of Eq. (3.110), we compute the maximum $\gamma \simeq 7$. From Fig. 3.7 we can see that for this value the chirality parameter is only $\Delta\chi \simeq 0.05$, hence no significant production of sourced gauge fields has taken place. While this does not preclude the existence of a realization of this model, leading to significant r and $n_T > 0$, it demonstrates that this requires some level of parameter fine-tuning.